Environmental Science and Pollution Research (2020) 27:15325–15336
https://doi.org/10.1007/s11356-020-08035-5

RESEARCH ARTICLE

Response of ecosystem functioning to environmental variations in an artificial sand-binding vegetation desert in northwestern China

Yuanyuan Zhou [1,2] · Xinrong Li [1] · Yanhong Gao [1] · Yanli Wang [1,2] · Zhongchao Mao [1,2]

Received: 12 October 2019 / Accepted: 10 February 2020 / Published online: 19 February 2020

Abstract

The establishment of artificial sand-binding vegetation is one of the main means for restoring damaged ecosystems that are impacted by global change. This study was conducted to evaluate the influence of environmental factors on ecosystem function (net ecosystem exchange (NEE), evapotranspiration (ET), and water use efficiency (WUE)) in an artificial sand-binding vegetation desert (with dominant shrubs, such as *Artemisia ordosica* and *Caragana korshinskii*, and herbaceous plants) in northwestern China. NEE, ET, and meteorological data were observed with the eddy covariance (EC) technique. The random forest (RF) method was used to identify major environmental factors that affected NEE, ET, and WUE. Our results showed that the mean annual NEE, ET, and WUE values were − 112.4 g C m^{-2}, 232.1 mm, and 0.49 g C kg^{-1} H_2O, respectively, during the 2015 to 2018 growing seasons. At the weekly scale, the most important drivers of NEE were the normalized difference vegetation index (NDVI) and soil water content (SWC). Rainfall, SWC, and NDVI were important drivers of ET. WUE was mainly controlled by rainfall and SWC. Linear regression showed that NEE had significant negative relationships with the NDVI and SWC. ET had positive relationships with rainfall, SWC, and the NDVI. WUE had significant negative relationships with SWC and rainfall. These findings indicate that drought inhibited ET more than carbon absorption, thus promoting the WUE of the ecosystem to some extent. The close relation of the ecosystem function to SWC implies that this ecosystem may be critically regulated by future climate change (specifically, changes in rainfall patterns).

Keywords Artificial sand-binding vegetation · Eddy covariance · Random forest · Net ecosystem exchange · Evapotranspiration · Water use efficiency

Introduction

The area affected by windblown sand hazards in northern China covers approximately 3.2×10^5 km^2 (Li et al. 2014). Reconstructing and restoring vegetation are important and effective ways to mitigate sandstorm hazards and control desertification (Le Houérou 2000). Artificial sand-binding vegetation has been established over 6×10^6 ha of windblown sand hazard areas in northern China (Wang et al. 2007; Cao et al. 2011). Large-scale plantations have significantly increased local carbon stock storage and reduced the concentration of carbon dioxide in local areas (Liang et al. 2006; Gao et al. 2012; Yang et al. 2014). However, carbon sequestration by plantations in the region often requires large amounts of water, posing potential risks to the health of local ecosystems (Farley et al. 2005). Water stress has become the main influencing factor affecting the stability of artificial vegetation. The contrast between carbon sequestration by plantations and the scarcity of water resources has become increasingly prominent (Li

Responsible editor: Philippe Garrigues

✉ Xinrong Li
lxinrong@lzb.ac.cn

Yuanyuan Zhou
yyzhou2011@lzu.edu.cn

Yanhong Gao
gao_yanhong@lzb.ac.cn

Yanli Wang
wangyanli126@hotmail.com

Zhongchao Mao
shzcmao@163.com

[1] Shapotou Desert Research and Experiment Station, Northwest Institute of Eco-Environment and Resources, Chinese Academy of Sciences, Lanzhou 730000, China

[2] University of Chinese Academy of Sciences, Beijing 100049, China

et al. 2013). Currently, it is of great significance to explore the processes and mechanisms of water and carbon exchange in artificially vegetated lands to comprehensively assess the ecological and environmental benefits of sand control and scientifically guide afforestation and desert ecosystem management activities (Li et al. 2014; Zhang and Jin 2016).

Net ecosystem exchange (NEE), evapotranspiration (ET), and water use efficiency (WUE) are the three key parameters that reflect the functioning of ecosystems. NEE refers to the absorbance of CO_2 by plants to balance plant and soil respiration. Net ecosystem productivity (NEP = – NEE) reflects the production capacity of an ecosystem and is highly sensitive to climate change and human activities (Han et al. 2013). ET is the sum of water that is lost to the atmosphere from the soil surface through evaporation and from plant tissues via transpiration, and ET is also a vital component of the water cycle (Mu et al. 2007). ET is the main form of water loss in arid lands, and the balance between precipitation and ET is crucial for determining ecosystem structure, function, and productivity (Eldridge et al. 2016; Liu et al. 2016). WUE, the ratio of NEP to ET, reflects how efficiently plants use water to produce biomass and is used as an indicator of the suitability of an environment for plant growth (Hamerlynck et al. 2014). Analysing the variability in WUE can improve our understanding of the interaction between carbon and water cycles at a large scale and provide a basis for improving regional carbon sequestration and water use budget assessments (Zhu et al. 2015; Khalifa et al. 2017). Therefore, studies on NEE, ET, and WUE are particularly important in dry areas (Huang and Luo 2017).

The eddy correlation (EC) method can be used to determine CO_2 and H_2O exchange in an ecosystem at a high temporal resolution and continuously monitor WUE. This method provides an effective means for studying the temporal dynamics of NEE, ET, and WUE and their responses to environmental change at different time scales (Law et al. 2002). Studies have found that many environmental factors (including biological and abiotic factors) affect carbon and hydrological cycle processes. In general, the environmental factors that affect NEE include solar radiation, temperature, precipitation, soil moisture, vapour pressure deficit (VPD), soil nutrients, and ground cover characteristics (Zhao and Running 2010; Li et al. 2016a). The environmental factors involved in ET are precipitation, wind velocity, solar radiation, humidity, air temperature, etc. (Liu and Feng 2012). While other studies found that the responses of both ET and NEE to environmental factors at a monthly scale were consistent, the responses were controlled by biological factors via changes in surface conductance (Steduto et al. 2007; Zhao et al. 2007; Tong et al. 2014). The environmental variables impacting ecosystem WUE include photosynthetically active radiation (PAR), net radiation (Rn), VPD, air temperature, precipitation, soil water content (SWC), leaf area index (LAI), and normalized difference vegetation index (NDVI), which were found to be mostly intercorrelated (Tong et al. 2014; Xie et al. 2016; Lin et al. 2018). In addition, ecosystems differ in their responses to climate variability (Knapp and Smith 2001; Khalifa et al. 2017), and the same site responds differently to environmental factors at different time scales (Law et al. 2002). However, studies on the responses of NEE, ET, and WUE to environmental factors in arid regions are rare.

The protected area in the Shapotou section of the Baotou-Lanzhou railway is a typical representative of artificial vegetation construction in a Chinese desert (Fig. 1). This area is

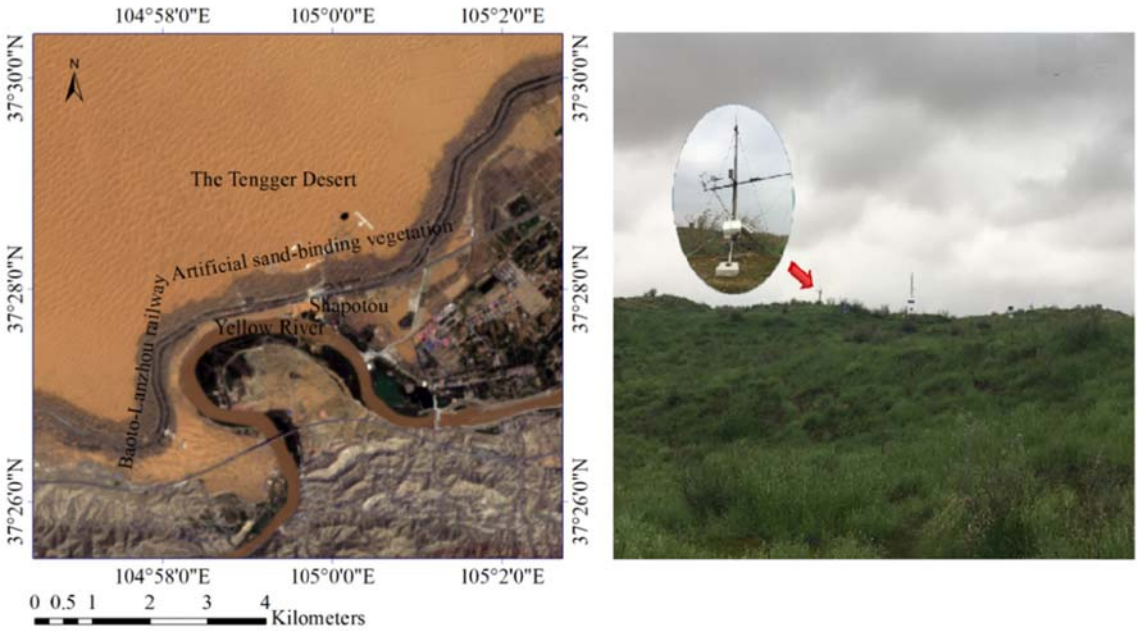

Fig. 1 The artificial sand-binding vegetation area of the Tengger Desert, China

located at a great distance inland, with sparse vegetation, high temperatures, strong radiation, and rare annual precipitation with large fluctuations. Precipitation in this area is the only source of ecosystem moisture because the groundwater level in this area is too low (approximately − 60 m) for the plants to use (Li et al. 2007b). This ecosystem protects the area against wind and sand and serves as a typical study area for ecological-hydrological function research in arid regions. However, at present, research on NEE, ET, and WUE in the region has mostly involved single parameters and has been conducted at the leaf level or plant level for major species (Wang et al. 2010; Gao et al. 2012; Bao et al. 2015; Chen et al. 2015; Gao et al. 2015), and comprehensive research on the ecological-hydrological function response to the environment has not yet been conducted. For this reason, the relationships of NEE, ET, and WUE in the artificial sand-binding vegetation area with environmental variables are unclear. Hence, how do NEE, ET, and WUE dynamics change with changes in environmental factors, and which factors are the most important? How do these factors affect these dynamics? Therefore, the study of how environmental factors affect NEE, ET, and WUE is critical to the sustainable development of this ecosystem.

Scholars have used correlation analysis (Kutzbach et al. 2015); partial correlation analysis (Fu et al. 2009); one-factor linear regression (Li et al. 2016b); multiple stepwise regression (Wohlfahrt et al. 2008); structural equation modelling (Quan et al. 2018; Zhang et al. 2018); redundancy analysis (Fei et al. 2018); principal component analysis (Swann and Fung 1998), wavelet transform, wavelet coherence, and partial wavelet coherence analysis (Jia et al. 2018); and random forest (RF) analysis to analyse the relationships between carbon or water fluxes and environmental variables. The RF algorithm is a popular machine learning algorithm and is similar to multiple linear regression but often outperforms multiple regression models and can predict data that include multiple high-order interaction terms (Mutanga et al. 2012; Liu et al. 2018). The RF algorithm has the characteristics of strong noise immunity and strong resistance to overfitting and underfitting. RFs are also simple to train, can handle a large amount of mixed-type data and provide ways to evaluate variable importance scores (Pham and Brabyn 2017; Torres-García and Domenech 2017; Wei et al. 2017). However, RF algorithms have not been used to analyse carbon-hydrological interactions in desert environments. In this paper, based on EC observations, the carbon flux, ET, and meteorological factors were continuously measured in an artificial sand-binding vegetation area in the southeastern Tengger Desert for four and a half growing seasons. We used the RF method and linear regression to investigate the environmental factors driving NEE, ET, and WUE. The objectives of this study were to (i) examine the magnitudes of the carbon flux, ET, and WUE during the growing season and (ii) identify the environmental variables controlling the NEE, ET, and WUE at weekly scales during the growing season. Quantitative evaluations of NEE, ET, and WUE and the underlying environmental controls are also crucial for predicting future climate change impacts on ecosystem carbon-water interactions.

Materials and methods

Site description

The observations were conducted during the 2014–2018 growing seasons throughout the northern region of the artificial vegetation area (planted in 1956) around the Shapotou Experimental Station (37° 28′E, 105° 0′N, 1320 m above sea level), which belongs to the Chinese Academy of Sciences in the Ningxia Hui Autonomous Region and is located at the southeastern margin of the Tengger Desert (Fig. 1). The site is typical of an ecotone between a desertified steppe and sandy desert, and this area is also a transitional zone between sandy and revegetated deserts. The annual mean temperature is 9.6 °C. The mean, maximum, and minimum annual precipitation are approximately 186, 304, and 88 mm, respectively, 80% of which falls between May and September (1956 to 2003). The potential evaporation is 3000 mm, and the mean relative humidity is 40%. The average wind speed is 2.8 m s^{-1}. The soil surface is loose and comprises poorly aggregated mobile sand with a moisture content of 2 to 3% (Huang et al. 2014). The mean volumetric SWC in the 0–300 cm deep layers of the revegetated sites ranges from approximately 0.8 to 3.3% (Li et al. 2014). The vegetation is dominated by shrubs, such as *Artemisia ordosica* and *Caragana korshinskii*, and herbaceous plants, such as *Echinops gmelinii*, *Cornulaca alaschanica*, *Bassia dasyphylla*, *Setaria viridis*, *Eragrostis minor*, and *Corispermum hyssopifolium* (Li et al. 2014). The shrub and herb coverages are 8–10% and 30–45%, respectively (Li et al. 2014).

Experimental observation system

EC measurements began at the site in July 2014. The system consisted of an open path infrared gas analyser (Li-7500A, Li-Cor, Lincoln, NE, USA) and a three-dimensional sonic anemometer (CST3, Campbell Scientific, Logan, UT, USA) mounted at a height of 2 m. The former measured the molar densities of CO_2 and water vapour, whereas the latter measured instantaneous fluctuations in the three-dimensional (vertical, streamwise, and lateral) wind speed and virtual temperature. The data were measured at 10 Hz. The installation setup of additional meteorological instruments is shown in Table 1. All flux data and meteorological factors were recorded with a data logger (9210, Sutron, USA).

Table 1 Installation setup of additional meteorological instruments

Measuring element	Instrument model	Installation location (cm)
Net radiation (Rn)	K&Z, CNR4, Delft, Netherlands	150
Photosynthetic photon flux density (PPFD)	LI-109, Li-Cor, USA	150
Air temperature and air humidity (Ta and RH)	HMP155, Vaisala, Finland	150
Soil temperature and soil water content (Ts and SWC)	70030, Stevens, USA	− 5, − 10, − 20, − 40, − 60
Soil heat flux	HFP01SC-10, Hukseflux, USA	− 5
Precipitation	TR-525 MM, TE, USA	50

Data processing and WUE calculation

The raw greenhouse gas (GHG) data were processed with EddyPro 6.0 (Li-cor) software. The carbon and water vapour fluxes were obtained 30 min after tilt correction (secondary coordinate rotation); sonic virtual temperature correction; Webb, Pearman and Leuning (WPL) correction; turbulent fluctuation blocking; time lag compensation; spike detection and removal; and other statistical tests and spectral corrections. Then, values that were unstable due to rainfall, snow, fog, sensor malfunction, and maintenance, human-induced effects, and insufficient turbulence (at night) were eliminated. We filtered the original night-time dataset when $u^* < 0.2$ m s^{-1}. The u^* threshold was estimated following the ChinaFLUX standard method (Zhu et al. 2006). The total NEE and ET values in the study period were filtered out at approximately 19.48% and 9.74%, respectively. Consequently, 10.7% and 5.4% of the total daytime NEE and ET needed to be gap-filled compared to proportions of 30.8% and 15.3% at night-time, respectively. To fill these gaps, we applied the mean diurnal variation (MDV) (Falge et al. 2001) and interpolation (Baldocchi 2003; Austin et al. 2004; Xu and Baldocchi 2004) methods. WUE is an important indicator of the characteristics of the water–carbon coupling process. In this paper, we used conventional methods to calculate ecosystem WUE (Law et al. 2002; Emmerich 2007).

$$WUE = NEP/ET = -NEE/ET \quad (1)$$

Obtaining NDVI data

The NDVI is an alternative measurement of vegetation canopy that is associated with the LAI and percentage of vegetation cover (Nagler et al. 2005). The MODIS daily 250 m NDVI was calculated with the Google Earth engine (https://earthengine.google.com/) with an online subset output of a 250 × 250 m pixel subset that was centred on the flux site. The growth state of the vegetation is difficult to determine based on the NDVI because vegetation is sparse in deserts; therefore, NDVI values less than 0.1 were not included in the statistical analysis (Song et al. 2010).

Random forest analysis

We conducted a RF analysis (Breiman 2001) to screen and determine the major drivers of carbon fluxes among environmental variables (i.e. PPFD, Ta, Ts, VPD, rainfall, average SWC, and NDVI). Because the coarse roots of *Artemisia ordosica* and *Caragana korshinskii* were concentrated in the upper 0.6 m of the soil (Zhang et al. 2008, 2009), we calculated the average SWC at depths of 5, 10, 20, 40, and 60 cm. RF extends standard classification and regression tree methods by creating a collection of classification trees by binary divisions (Delgado-Baquerizo et al. 2016; Pham and Brabyn 2017). The fit of each tree is evaluated by using randomly selected points that cover 1/3 of the data, and the remaining 2/3 of the data are included in a bootstrap sample (Pham and Brabyn 2017). The importance of each factor is determined by assessing the increase in the mean square error between observations and predictions; the data for modelling are randomly permuted (Delgado-Baquerizo et al. 2016). Among the different iterations, the order of importance of the important variables remains stable, but the order of the less important variables is not. The stability and generalization of the model and the cross-validated R^2 and root mean square error (RMSE) were also assessed. The RF analysis parameters were set to 1000 decision trees (ntree), 5 random subsets of the predictors (mtry), and a node size of 5.

Statistical analysis

We used MATLAB to eliminate and interpolate the flux data and meteorological data. The RF method (R language 3.4.4) was used to determine the most important environmental factors affecting NEE, ET, and WUE. Linear regression (SPSS Inc., Chicago, IL, USA) was used to determine the relationships among NEE, ET and WUE and the responses of ecosystem functional factors to the main environmental factors. All figures were drawn with Origin 8.5 (OriginLab, USA).

Energy balance closure

The energy non-closure phenomenon is prevalent at EC observation sites, and the energy closure range is

generally 55–90% (Wilson et al. 2002). In this study, the degree of energy closure (sensible heat (H) + latent heat (LE) versus net radiation (Rn) − soil heat flux (G)) was 0.68 throughout the study period, indicating that the observed data quality met the observation requirements.

Results

Seasonal variations in the abiotic and biotic environmental variables

Figure 2 and Table 2 display the weekly mean values or the accumulation of biotic and abiotic variables during the growing season. The average weekly PPFD, VPD, Ta, and Ts values exhibited approximate unimodal trends and peaked in June or July. Significant seasonal dynamics were found, varying from 719.37 μmol m^{-2} s^{-1} in June 2015 to 39.47 μmol m^{-2} s^{-1} in October 2017, 4.31 kPa in July 2017 to 0.0007 kPa in April 2016, 34.15 °C in July 2017 to 1.3 °C in October 2017, and 40.54 °C in July 2015 to 4.35 °C in October 2016 (Fig. 2). During the 2015 to 2018 growing seasons, the average PPFD, VPD, Ta, and Ts were 427.8 μmol m^{-2} s^{-1}, 1.08 kPa, 20.1 °C, and 24.6 °C, respectively (Table 2). There were large differences in the amount and distribution of single growing season rainfall and interannual rainfall (Fig. 2 and Table 2). The variation in SWC was closely related to rainfall patterns, and the average SWC was 3.04% (Table 2). The NDVI was significantly lower in 2015 than in other years. The average weekly NDVI was 0.21 and peaked at 0.39 in September (Fig. 2 and Table 2).

Dynamics of NEE, ET, and WUE and the relationships among them

The weekly NEE, ET, and WUE variations at seasonal and interannual timescales were remarkable, with maximum values of −16.69 g C m^{-2} wk^{-1}, 23.77 mm wk^{-1}, and 2.3 g C kg^{-1} H_2O, respectively (Fig. 3). During the growing season, both NEE and ET reached a maximum in the wet season in 2018, and WUE reached its maximum during a drought in 2015 (Table 2). From 2015 to 2018, the cumulative annual growing season average NEE, ET, and WUE values were −112.4 g C m^{-2}, 232.1 mm, and 0.49 g C kg^{-1} H_2O, respectively (Table 2). There was a good relationship between NEE and ET, and NEE decreased as ET increased (Fig. 4).

The effect of environmental variables on NEE, ET, and WUE

The variable importance (defined as the interpretation of the contributions to NEE, ET, and WUE) rankings from the RF analysis are shown in Figs. 5 and 6 show the goodness of fit measure of the RF analysis. The results indicated that for NEE during the growing season, the NDVI was the most important variable, with an average increase in the mean square error (MSE) of 3.97%, followed by SWC; these variables were significant at the 0.01 and 0.05 levels, respectively (Fig. 5a). Rainfall, SWC and the NDVI were significant at the 0.01 level and 0.05 level for predicting ET (Fig. 5a). For WUE, the most important variables were rainfall and SWC (Fig. 5b).

Regression analysis (Fig. 7) provided further insight into the direction of the relationships between the major environmental variables and NEE, ET, and WUE. The NDVI was used as a proxy for canopy development in this study. Both

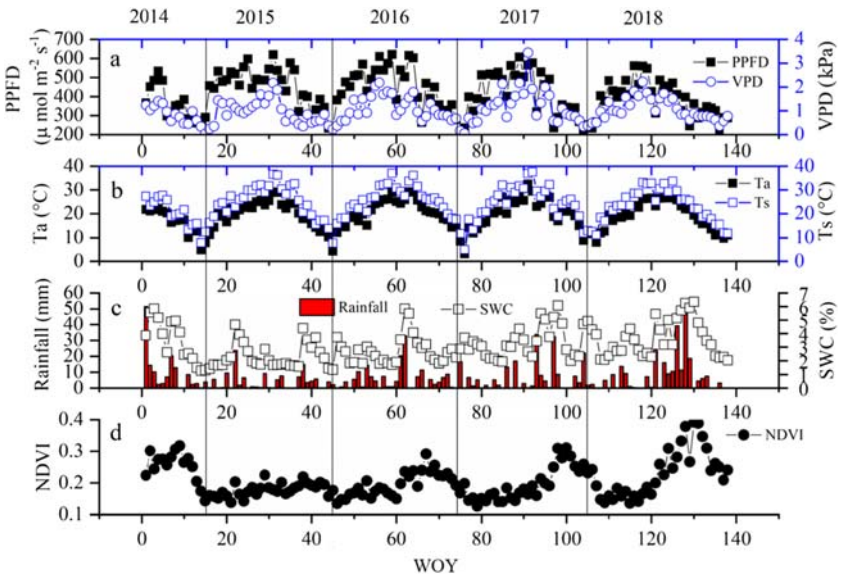

Fig. 2 Average weekly variations in the **a** photosynthetic photon flux density (PPFD) and vapour pressure deficit (VPD); **b** air temperature (Ta) and soil temperature at 5 cm (Ts); **c** soil water content (SWC, depths of 5, 10, 20, 40, and 60 cm), and weekly total rainfall; and **d** NDVI during the 2014 to 2018 growing seasons (from April to October). For the x-axis, the data refer to the week of the year (WOY, seven-day periods) and range from 1 to 138

Table 2 Interannual variability in the average PPFD, VPD, Ta, Ts, SWC, and NDVI, total rainfall, cumulative ET, NEE, and WUE in the 2014 to 2018 growing seasons ± SE (standard error)

	PPFD	VPD	Ta	Ts	Rainfall	SWC	NDVI	NEE	ET	WUE
	μmol m^{-2} s^{-1}	kPa	°C	°C	mm	%		g C m^{-2}	mm	g C kg^{-1} H_2O
2014	373.6 ± 15.96	0.9 ± 0.06	17.8 ± 0.50	21.4 ± 0.59	135.1	3.79 ± 0.16	0.27 ± 0.007	− 73.2	115	0.64
2015	452.0 ± 11.19	0.9 ± 0.05	19.7 ± 0.42	24.7 ± 0.50	117.5	2.31 ± 0.065	0.18 ± 0.003	− 117.5	196.5	0.60
2016	448.6 ± 11.00	1.1 ± 0.05	20.4 ± 0.43	25.1 ± 0.50	176.3	2.76 ± 0.075	0.20 ± 0.003	− 98.9	231.5	0.43
2017	412.7 ± 11.06	1.2 ± 0.05	20.2 ± 0.45	24.3 ± 0.52	181.2	3.45 ± 0.03	0.19 ± 0.05	− 96.7	233.1	0.41
2018	397.9 ± 10.25	1.12 ± 0.04	19.92 ± 0.42	24.22 ± 0.45	246.4	3.62 ± 0.051	0.23 ± 0.061	− 136.3	267.4	0.51
2015–2018 mean	427.8 ± 6.00	1.08 ± 0.03	20.06 ± 0.23	24.58 ± 0.27	180.35	3.04 ± 0.043	0.21 ± 0.009	− 112.35 ± 9.25	232.13 ± 14.48	0.49 ± 0.04

NEE and ET had significant linear relationships with the NDVI, and the NDVI explained 26% and 21% of the variation in NEE and ET throughout the study period, respectively (Fig. 7a and e). Strong negative and positive linear correlations of SWC and NEE with ET in the growing season were observed in this area, respectively (Fig. 7b and d). ET increased linearly with increasing rainfall, and rainfall explained 41% of the seasonal variation in ET (Fig. 7c). Unexpectedly, the increases in rainfall and SWC were inconsistent with the seasonal variation in WUE during the study period (Fig. 7f and g).

Discussion

Magnitudes of NEE, ET, and WUE during the growing season

The annual net C sinks ranged from − 96.7 to − 136.3 g C m^{-2}, with a mean annual NEE of − 112.35 ± 9.25 (mean ± SE) g C m^{-2} during the 2015–2018 growing seasons (Table 2). This finding means that the artificial sand-binding vegetation desert ecosystem acted as a carbon sink during the growing season. The cumulative annual growing season average ET was 232.1 ± 14.48 mm and increased as the annual rainfall amount increased (Table 2). Gao et al. (2012, 2015) reported that the NEE and ET of a 20-year-old revegetated area near our study site were − 18.6 g C m^{-2} y^{-1} and 166.9 mm y^{-1}, respectively. The weekly NEE exhibited a negative relationship with weekly ET (Fig. 4), indicating that relatively high net carbon uptake corresponded to high ET. The strong correlation between NEE and ET demonstrated that the carbon and water cycles were tightly coupled due to stomatal control for both carbon and water exchange between ecosystems and the atmosphere through photosynthesis and transpiration (Niu et al. 2008; Chapin et al. 2011). In general, high stomatal conductance leads to high transpiration and high photosynthesis (Mu et al. 2007).

The coupling of carbon and water cycles resulted in seasonal variations in WUE. A high WUE indicates that more photosynthetic products can be obtained with limited water resources (Beer et al. 2009; Yang et al. 2010). WUE fluctuated interannually in the artificial sand-binding vegetation desert (Table 2). The study area is typical of an ecotone between a desertified steppe and sandy desert; therefore, this area has the characteristics of both grassland and desert. The annual growing season average WUE from 2015 to 2018 was 0.49 ± 0.04 g C kg^{-1} H_2O, which was lower than the values reported by Huang and Luo (2017) for grasslands in northern China (0.56 g C kg^{-1} H_2O). The value was also lower than the values reported in other studies on grasslands (e.g. Han et al. 2013). However, our results were higher than the values obtained at the DangXiong (0.36 g C kg^{-1} H_2O) and Xilinhot (0.45 g C kg^{-1} H_2O) sites (Wang et al. 2008; Zhu et al. 2015). Previous

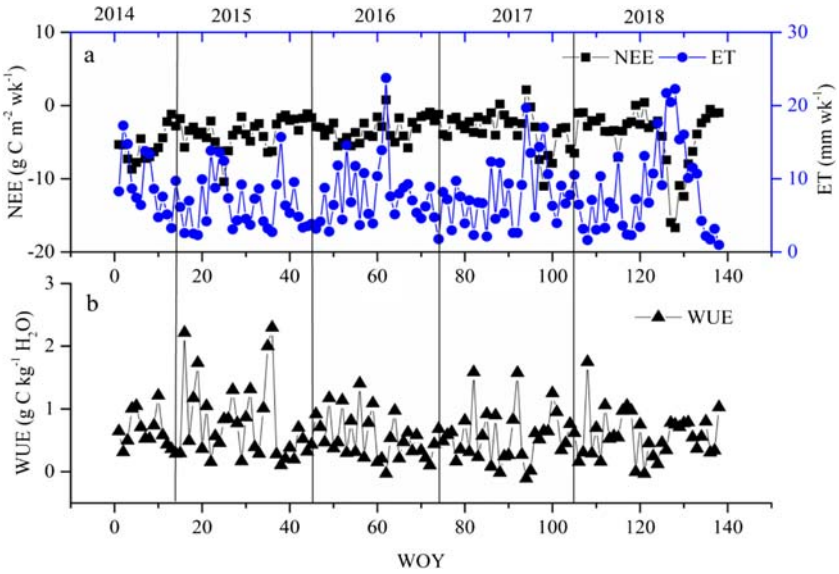

Fig. 3 Dynamics of weekly **a** NEE (negative values indicate CO_2 assimilation by the ecosystem and, vice versa) and ET and **b** WUE

studies reported that WUE estimates from grassland sites generally ranged from 0.47 to 2.76 g C kg^{-1} H_2O (Zhu et al. 2015), and our results fell within this range. Our results were higher than the values reported by Liu et al. (2012), who obtained desert halophyte community ecosystem WUE values of 0.03 and 0.15 g C kg^{-1} H_2O in dry and wet years, respectively. Essentially, WUE varies with the type of terrestrial ecosystem and differs greatly depending on location, climatic factors, vegetation characteristics and disturbance regime (Ponton et al. 2006; Hu et al. 2008). However, the WUE values of the dominant plants, *Artemisia ordosica* and *Caragana korshinskii*, were 1.2~3.4 and 0.6~3.0 g C kg^{-1} H_2O, respectively (Bao et al. 2015; Fu et al. 2015), which were larger than the ecosystem WUE values. This result was due to the large amount of open space in the study area, and the evaporation of soil accounted for a large proportion.

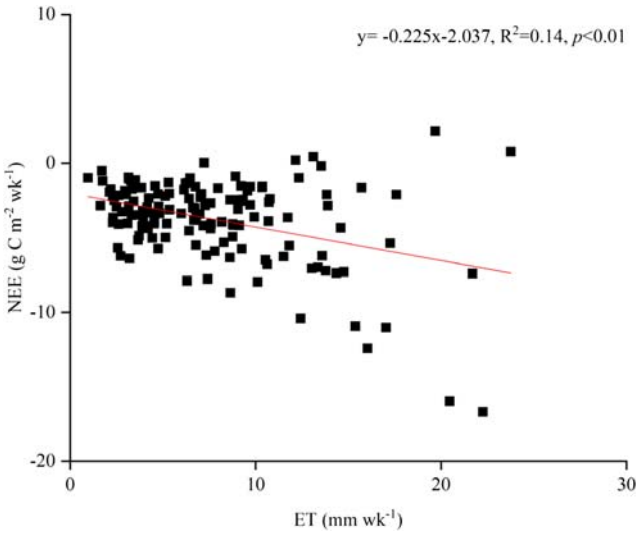

Fig. 4 The relationships between weekly ET and NEE

Effects of environmental variables on NEE, ET, and WUE

NEE, ET, and WUE are controlled by canopy architecture and development, soil characteristics, and a variety of in situ environmental variables (Kelliher et al. 1995; Wilson et al. 2002). Here, we used RFs to explain the factors with the most important influence. RFs are able to not only perform regressions but also make predictions. In our RF models, the parameters made the errors of the models converge to a minimum and reach stability, which may be an indication that the generalization requirements of RF models were met (Liu et al. 2018, Fig. 6). Thus, the RF models provided good estimates of NEE, ET, and WUE and were able to explain most of the variations in NEE, ET, and WUE during the study period. RF analysis showed that the most important factors affecting NEE were the NDVI and SWC (Fig. 5a). Rainfall, SWC, and the NDVI played vital roles in predicting ET (Fig. 5a). Rainfall

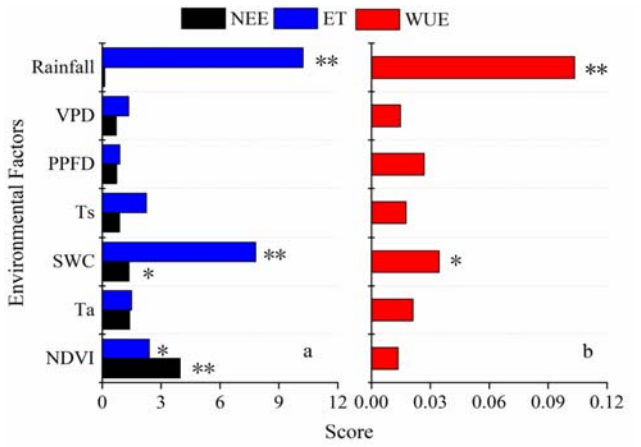

Fig. 5 Important values (score). ** and * represent significance levels of 0.01 and 0.05, respectively

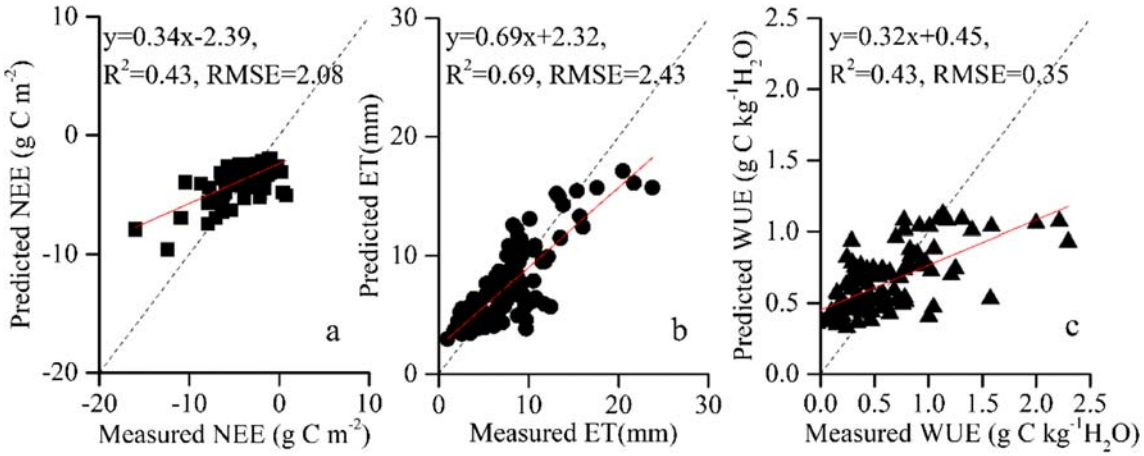

Fig. 6 Scatterplots of weekly **a** NEE, **b** ET, and **c** WUE between observations and predictions during the 2014 and 2018 growing seasons. The dashed black lines and red lines represent the 1:1 line and linear fit, respectively

and SWC also regulated WUE significantly (Fig. 5b). These results were all at the weekly scale.

NEE and ET were controlled by the NDVI. NEE and ET had negative and positive linear relationships with the NDVI, respectively (Fig. 7a and e). The NDVI is a metric of greenness that is indicative of the number of green leaves and is quantified by the LAI (Liu et al. 2019). Thus, we concluded that variations in NEE and ET were probably due to plant controls on canopy conductance and the NDVI (LAI). Therefore, canopy architecture and the development and soil moisture conditions acted as major constraints on the NEE and ET. Moreover, variation in the NDVI was associated with differences in soil water availability for plants (Fig. 8). This finding indicates that the most influential factor for both variables was soil moisture.

In arid and semiarid regions, soil moisture acts as a mutual transmission link connecting precipitation, surface water, and groundwater, affecting water, energy, and earth biochemical

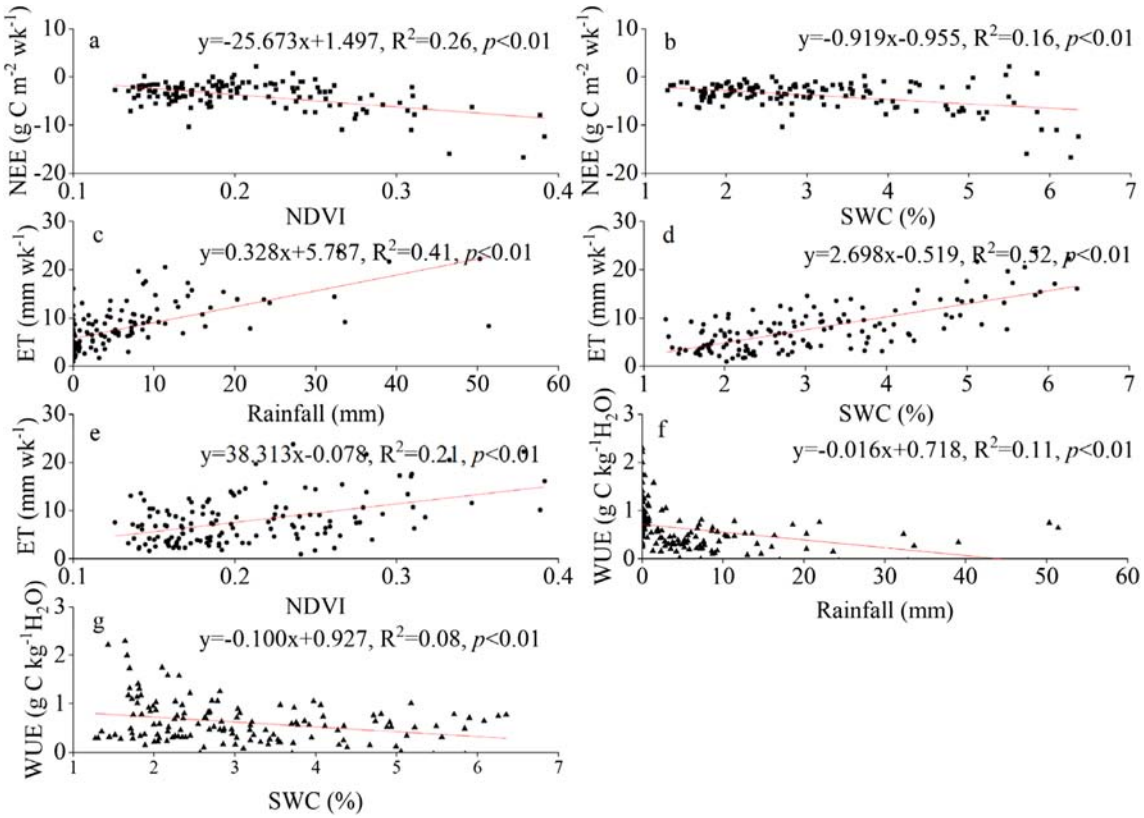

Fig. 7 The relationships between the major weekly environmental variables and **a** and **b** NEE, **c**, **d**, and **e** ET, and **f** and **g** WUE during the 2014–2018 growing seasons

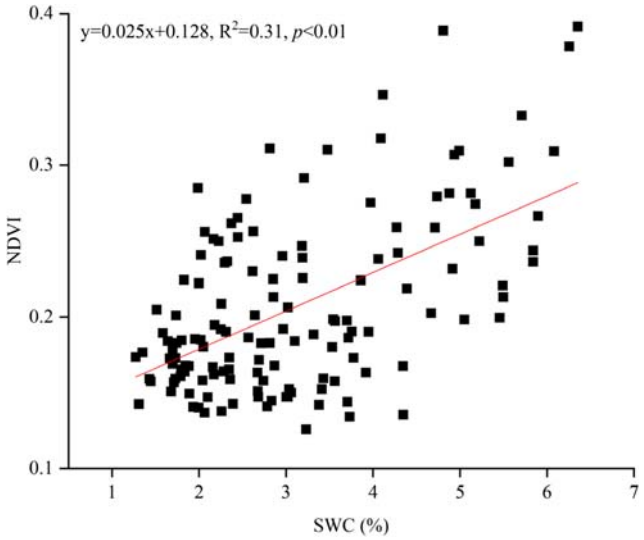

Fig. 8 The relationship between weekly mean SWC and NDVI

cycles by restricting ET and photosynthesis (Oki and Kanae 2006). In this study, the CO_2 flux was negatively related to the volumetric SWC during the growing season (Fig. 7b). This result suggests that NEE decreases with soil moisture and that a high soil water content can promote the absorption of carbon in this ecosystem. This phenomenon is more common in arid and semiarid regions (e.g., Itoh et al. 2012). Our results showed that ET was strongly, positively, linearly correlated with rainfall and SWC (Fig. 7c and d). This finding indicates that high amounts of rainfall and SWC can promote vegetation transpiration or soil evaporation. The close relationships of ET with rainfall and SWC were consistent with the results reported by Li et al. (2007a) on a Mongolian steppe, Sala et al. (1992) on a shortgrass steppe and Noy-Meir (1973) in desert ecosystems. WUE is the link between NEE and ET, and factors affecting both will inevitably affect WUE. Various studies have shown that WUE often increases as water availability decreases in dryland ecosystems (Ehleringer and Cooper 1988; Toft et al. 1989; Sheng et al. 2011). Our results were consistent with this phenomenon (Fig. 7f and g). The reason that WUE decreased with SWC and rainfall may be because SWC and rainfall had a greater effect on ET than NEE because ET increased more rapidly than NEP (-NEE) as the SWC increased (Fig. 7b–d). Increases in WUE during droughts mainly result from internal mechanisms of stomata that work to reduce water losses for adapting to water stress (Reichstein et al. 2002). However, Liu et al. (2012) found that WUE in a wet year was greater than that in a dry year in a desert halophyte community in western China, which contrasted with our findings. This difference was because the groundwater level where the aforementioned study was conducted was shallow, the main shrubs were less dependent on rainfall, and there were more annual or ephemeral plants; this scenario resulted because the community structure adjusted and used the extra precipitation water input in the wet year, and consequently, the community productivity increased. That is, as water becomes increasingly scarce, ecosystems increasingly devote more resources to maximizing the efficient use of water (Huxman et al. 2004; Bai et al. 2008; Troch et al. 2009). Global climate models predict that future precipitation patterns at mid-latitudes may be strengthened further, as evidenced by increases in total precipitation, increases in drought durations, and increases in the frequency of extreme precipitation events (Huntington 2006; IPCC 2007). These conditions will have profound impacts on the functions of artificial sand-binding vegetation ecosystems.

Although the RF algorithm provided good estimates of NEE, ET, and WUE (Fig. 6), the accuracy of the RF model was influenced by the quality of the input flux data because the method used to fill the gaps in flux data increased the error of the model to some extent. Therefore, it took a long time to observe the accuracy of the results.

Conclusions

Observations of CO_2 and H_2O fluxes using the EC technique accurately quantified the carbon uptake and water consumption capacity of the Shapotou artificial revegetation area. The figures show the ecosystem performance in the growing season in our study period and the absorption of CO_2. NEE was mainly driven by the NDVI and SWC during the study period. The NDVI was also significant for predicting ET. Changes in SWC and rainfall were the most important environmental factors controlling the dynamics of ET and WUE. NEE and ET had significant negative and positive linear relationships with the NDVI and SWC, respectively. ET also had positive linear relationships with the rainfall amount. WUE had negative linear relationships with rainfall and SWC. These findings indicated that a high SWC facilitated the ecosystem uptake of CO_2 and ET ability. Meanwhile, the high SWC would decrease the WUE ability because it had a greater effect on ET than NEE in this ecosystem. The close relation of SWC with ecosystem function implies that this ecosystem may be critically regulated by future climate change (specifically, changes in rainfall patterns).

Funding information Financial support was provided by the Natural Science Foundation of China (41530746 and 41621001).

References

Austin AT, Laura Y, Stark JM et al (2004) Water pulses and biogeochemical cycles in arid and semiarid ecosystems. Oecologia 141:221–235. https://doi.org/10.1007/s00442-004-1519-1

Bai YF, Wu JG, Xing Q, Pan QM, Huang JH, Yang DL, Han XG (2008) Primary production and rain use efficiency across a precipitation

gradient on the Mongolia Plateau. Ecology 89:2140–2153. https://doi.org/10.1890/07-0992.1

Baldocchi DD (2003) Assessing ecosystem carbon balance: problems and prospects of the eddy covariance technique. Glob Chang Biol 9:479–492

Bao JT, Wang J, Li XR, Zhang ZS, Su JQ (2015) Age-related changes in photosynthesis and water relations of revegetated *Caragana korshinskii* in the Tengger desert, Northern China. Trees 29:1749–1760. https://doi.org/10.1007/s00468-015-1255-7

Beer C, Ciais P, Reichstein M et al (2009) Temporal and among-site variability of inherent water use efficiency at the ecosystem level. Glob Biogeochem Cy 23:GB2018. https://doi.org/10.1029/2008GB003233

Breiman L (2001) Random forest. Mach Learn 45(1):5–32. https://doi.org/10.1023/A:1010933404324

Cao SX, Chen L, Shankman D, Wang CM, Wang XB, Zhang H (2011) Excessive reliance on afforestation in China's arid and semi-arid regions: lessons in ecological restoration. Earth Sci Rev 104:240–245. https://doi.org/10.1016/j.earscirev.2010.11.002

Chapin FS, Matson PA, Mooney HA (2011) Principles of terrestrial ecosystem ecology. Springer, New York

Chen D, Zhou HY, Li PG, Chen YL, Wang YL, Zhao X (2015) Circadian variations and regulation mechanism of eco-physiological characteristics of *Artemisia ordosica* and *Caragana korshinskii*. J Desert Res 35(6):1549–1556. https://doi.org/10.7522/j.issn.1000-694X.2015.00031 (in Chinese)

Delgado-Baquerizo M, Maestre FT, Reich PB, Jeffries TC, Gaitan JJ, Encinar D, Berdugo M, Campbell CD, Singh BK (2016) Microbial diversity drives multifunctionality in terrestrial ecosystems. Nat Commun 7:10541. https://doi.org/10.1038/ncomms10541

Ehleringer JR, Cooper TA (1988) Correlations between carbon isotope ratio and microhabitat in desert plants. Oecologia 76:562–566. https://doi.org/10.1007/BF00397870

Eldridge DJ, Poore AG, Ruiz-Colmenero M, Letnic M, Soliveres S (2016) Ecosystem structure, function, and composition in rangelands are negatively affected by livestock grazing. Ecol Appl 26:1273–1283. https://doi.org/10.1890/15-1234

Emmerich WE (2007) Ecosystem water use efficiency in a semiarid Shrubland and grassland community. Rangeland Ecol Manag 60(5):464–470. https://doi.org/10.2111/1551-5028(2007)60[464:EWUEIA]2.0.CO;2

Falge E, Baldocchi D, Olson R et al (2001) Gap filling strategies for defensible annual sums of net ecosystem exchange. Agric For Meteorol 107:43–69. https://doi.org/10.1016/S0168-1923(00)00225-2

Farley KA, Jobbágy EG, Jackson RB (2005) Effects of afforestation on water yield: a global synthesis with implications for policy. Glob Chang Biol 11:1565–1576. https://doi.org/10.1111/j.1365-2486.2005.01011.x

Fei XH, Song QH, Zhang YP, Liu Y, Sha L, Yu G, Zhang L, Duan C, Deng Y, Wu C, Lu Z, Luo K, Chen A, Xu K, Liu W, Huang H, Jin Y, Zhou R, Li J, Lin Y, Zhou L, Fu Y, Bai X, Tang X, Gao J, Zhou W, Grace J (2018) Carbon exchanges and their responses to temperature and precipitation in forest ecosystems in Yunnan, Southwest China. Sci Total Environ 616:824–840. https://doi.org/10.1016/j.scitotenv.2017.10.239

Fu Y, Zheng Z, Yu G et al (2009) Environmental influences on carbon dioxide fluxes over three grassland ecosystems in China. Biogeosciences 6(12):2879–2893. https://doi.org/10.5194/bg-6-2879-2009

Fu T, Jiang ZR, Bao JT, Zhu RQ, Lu YC (2015) Water and light use efficiency of 3 psammophytes in Shapotou area. J Gansu Agric Univ 2:106–110 (in Chinese)

Gao YH, Li XR, Liu LC, Jia RL, Yang HT, Gang L, Wei YP (2012) Seasonal variation of carbon exchange from a revegetation area in a Chinese desert. Agric For Meteorol 156:134–142. https://doi.org/10.1016/j.agrformet.2012.01.007

Gao YH, Liu LC, Jia RL, Yang HT, Gang L (2015) Evapotranspiration over artificially planted shrub communities in the shifting sand dune area of the Tengger Desert, north Central China. Ecohydrology 9:290–299. https://doi.org/10.1002/eco.1635

Hamerlynck EP, Scott RL, Cavanaugh ML, Barron-Gafford G (2014) Water use efficiency of annual-dominated and bunchgrass-dominated savanna intercanopy space. Ecohydrology 7:1208–1215. https://doi.org/10.1002/eco.1452

Han QF, Luo GP, Li CF, Ye H, Chen YL (2013) Modeling grassland net primary productivity and water-use efficiency along an elevational gradient of the northern Tianshan Mountains. J Arid Land 5:354–365. https://doi.org/10.1007/s40333-013-0182-y

Hu ZM, Yu GR, Fu YL et al (2008) Effects of vegetation control on ecosystem water use efficiency within and among four grassland ecosystems in China. Glob Chang Biol 14:1609–1619. https://doi.org/10.1111/j.1365-2486.2008.01582.x

Huang XT, Luo GP (2017) Spatio-temporal characteristics of evapotranspiration and water use efficiency in grasslands of Xinjiang. Chin J Plant Ecol 41:506–518. https://doi.org/10.17521/cjpe.2016.0142 (in Chinese)

Huang L, Zhang ZS, Li XR (2014) The extrapolation of the leaf area-based transpiration of two xerophytic shrubs in a revegetated desert area in the Tengger Desert, China. Hydrol Res 46:389–399. https://doi.org/10.2166/nh.2014.171

Huntington TG (2006) Evidence for intensification of the global water cycle: review and synthesis. J Hydrol 319:83–95. https://doi.org/10.1016/j.jhydrol.2005.07.003

Huxman TE, Smith MD, Fay PA, Knapp AK, Shaw MR, Loik ME, Smith SD, Tissue DT, Zak JC, Weltzin JF, Pockman WT, Sala OE, Haddad BM, Harte J, Koch GW, Schwinning S, Small EE, Williams DG (2004) Convergence across biomes to a common rain-use efficiency. Nature 429:651–654. https://doi.org/10.1038/nature02561

IPCC (2007) IPCC fourth assessment report-climate change 2007: the physical science basis. Cambridge University Press, Cambridge

Itoh M, Kosugi Y, Takanashi S et al (2012) Effects of soil water status on the spatial variation of carbon dioxide, methane and nitrous oxide fluxes in tropical rain-forest soils in peninsular Malaysia. J Trop Ecol 28:557–570. https://doi.org/10.1017/S0266467412000569

Jia X, Zha TS, Gong JN, Zhang YQ, Wu B, Qin SG, Peltola H (2018) Multi-scale dynamics and environmental controls on net ecosystem CO2 exchange over a temperate semiarid shrubland. Agric For Meteorol 259:250–259. https://doi.org/10.1016/j.agrformet.2018.05.009

Kelliher FM, Leuning R, Raupach MR, Schulze E-D (1995) Maximum conductances for evaporation from global vegetation types. Agric For Meteorol 73:1–16. https://doi.org/10.1016/0168-1923(94)02178-M

Khalifa M, Elagib NA, Ribbe L, Schneider K (2017) Spatio-temporal variations in climate, primary productivity and efficiency of water and carbon use of the land cover types in Sudan and Ethiopia. Sci Total Environ 624:790–806. https://doi.org/10.1016/j.scitotenv.2017.12.090

Knapp AK, Smith MD (2001) Variation among biomes in temporal dynamics of aboveground primary production. Science 291:481–484. https://doi.org/10.1126/science.291.5503.481

Kutzbach L, Wille C, Runkle B et al. (2015) Temperature drives interannual variability of growing season CO_2 and CH_4 fluxes of Siberian lowland tundra. In: Egu General Assembly Conference

Law BE, Falge E, Gu L et al (2002) Environmental controls over carbon dioxide and water vapor exchange of terrestrial vegetation. Agric For Meteorol 113:97–120. https://doi.org/10.1016/S0168-1923(02)00104-1

Le Houerou HN (2000) Restoration and rehabilitation of arid and semi-arid Mediterranean ecosystems in North Africa and West Asia: a

review. Arid Soil Res Rehab 14:3–14. https://doi.org/10.1080/089030600263139

Li SG, Asanuma J, Kotani A, Davaa G, Oyunbaatar D (2007a) Evapotranspiration from a Mongolian steppe under grazing and its environmental constraints. J Hydrol 333:133–143. https://doi.org/10.1016/j.jhydrol.2006.07.021

Li XR, Kong DS, Tan HJ, Wang XP (2007b) Changes in soil and vegetation following stabilisation of dunes in the southeastern fringe of the Tengger Desert, China. Plant Soil 300:221–231. https://doi.org/10.1007/s11104-007-9407-1

Li XR, Zhang ZS, Lei H, Wang XP (2013) Review of the ecohydrological processes and feedback mechanisms controlling sand-binding vegetation systems in sandy desert regions of China. Chin Sci Bull 58:1483–1496. https://doi.org/10.1007/s11434-012-5662-5

Li XR, Zhang ZS, Tan HJ, Gao YH, Liu LC, Wang XP (2014) Ecological restoration and recovery in the wind-blown sand hazard areas of northern China: relationship between soil water and carrying capacity for vegetation in the Tengger Desert. Sci China 57:539–548. https://doi.org/10.1007/s11427-014-4633-2

Li Z, Chen YN, Wang Y, Fang GH (2016a) Dynamic changes in terrestrial net primary production and their effects on evapotranspiration. Hydrol Earth Syst Sci 20:2169–2178. https://doi.org/10.5194/hess-20-2169-2016

Li HQ, Zhang FW, Li YN et al (2016b) Seasonal and inter-annual variations in CO_2 fluxes over 10 years in an alpine shrubland on the Qinghai-Tibetan Plateau, China. Agric For Meteorol 228-229:95–103. https://doi.org/10.1016/j.agrformet.2016.06.020

Liang ZS, Yang JW, Shao HB, Han RL (2006) Investigation on water consumption characteristics and water use efficiency of poplar under soil water deficits on the loess plateau. Colloid Surface B 53:23–28. https://doi.org/10.1016/j.colsurfb.2006.07.008

Lin YX, Grace J, Wei Z et al (2018) Water-use efficiency and its relationship with environmental and biological factors in a rubber plantation. J Hydrol 563:273–282. https://doi.org/10.1016/j.jhydrol.2018.05.026

Liu HZ, Feng JW (2012) Seasonal and interannual variations of evapotranspiration and energy exchange over different land surfaces in a semiarid area of China. J Appl Meteorol Clim 51:1875–1888. https://doi.org/10.1175/JAMC-D-11-0229.1

Liu R, Pan LP, Jenerette GD, Wang QX, Cieraad E, Li Y (2012) High efficiency in water use and carbon gain in a wet year for a desert halophyte community. Agric For Meteorol 162-163:127–135. https://doi.org/10.1016/j.agrformet.2012.04.015

Liu WB, Wang L, Zhou J et al (2016) A worldwide evaluation of basin-scale evapotranspiration estimates against the water balance method. J Hydrol 538:82–95. https://doi.org/10.1016/j.jhydrol.2016.04.006

Liu YL, Zhou GM, Du HQ et al (2018) Response of carbon uptake to abiotic and biotic drivers in an intensively managed Lei bamboo forest. J Environ Manag 223:713–722. https://doi.org/10.1016/j.jenvman.2018.06.046

Liu P, Zha TS, Jia X, Black TA, Jassal RS, Ma J, Bai Y, Wu Y (2019) Different effects of spring and summer droughts on ecosystem carbon and water exchanges in a semiarid shrubland ecosystem in Northwest China. Ecosystems 22:1–17. https://doi.org/10.1007/s10021-019-00379-5

Mu QZ, Heinsch FA, Zhao MS, Running SW (2007) Development of a global evapotranspiration algorithm based on MODIS and global meteorology data. Remote Sens Environ 111:519–536. https://doi.org/10.1016/j.rse.2007.04.015

Mutanga O, Adam E, Cho MA (2012) High density biomass estimation for wetland vegetation using WorldView-2 imagery and random forest regression algorithm. Int J Appl Earth Obs Geoinf 18:399–406. https://doi.org/10.1016/j.jag.2012.03.012

Nagler PL, Cleverly J, Glenn E, Lampkin D, Huete A, Wan Z (2005) Predicting riparian evapotranspiration from MODIS vegetation indices and meteorological data. Remote Sens Environ 94:17–30. https://doi.org/10.1016/j.rse.2004.08.009

Niu SL, Wu MY, Han Y, Xia JY, Li LH, Wan SQ (2008) Water-mediated responses of ecosystem carbon fluxes to climatic change in a temperate steppe. New Phytol 177:209–219. https://doi.org/10.1111/j.1469-8137.2007.02237.x

Noy-Meir I (1973) Desert ecosystems: environment and producers. Annu Rev Ecol Syst 4:25–51. https://doi.org/10.1146/annurev.es.04.110173.000325

Oki T, Kanae S (2006) Global hydrological cycles and world water resources. Science 313:1068–1072. https://doi.org/10.1126/science.1128845

Pham LTH, Brabyn L (2017) Monitoring mangrove biomass change in Vietnam using SPOT images and an object-based approach combined with machine learning algorithms. Isprs J Photogramm 128:86–97. https://doi.org/10.1016/j.isprsjprs.2017.03.013

Ponton S, Flanagan LB, Alstad KP et al (2006) Comparison of ecosystem water-use efficiency among Douglas-fir forest, aspen forest and grassland using eddy covariance and carbon isotope techniques. Glob Chang Biol 12(2):294–310. https://doi.org/10.1111/j.1365-2486.2005.01103.x

Quan Q, Zhang F, Tian D, Zhou Q, Wang L, Niu S (2018) Transpiration dominates ecosystem water use efficiency in response to warming in an alpine meadow. J Geophysl Res- Biogeo 123(2):453–462. https://doi.org/10.1002/2017JG004362

Reichstein M, Tenhunen JD, Roupsard O et al (2002) Severe drought effects on ecosystem CO_2 and H_2O fluxes at three Mediterranean evergreen sites: revision of current hypotheses? Glob Chang Biol 8(10):999–1017. https://doi.org/10.1046/j.1365-2486.2002.00530.x

Sala OE, Lauenroth WK, Parton WJ (1992) Long-term soil water dynamics in the shortgrass steppe. Ecology 73:1175–1181. https://doi.org/10.2307/1940667

Sheng WP, Ren SJ, Yu GR, Fang HJ, Jiang CM, Zhang M (2011) Patterns and driving factors of WUE and NUE in natural forest ecosystems along the north-south transect of eastern China. J Geogr Sci 21:651–665. https://doi.org/10.1007/s11442-011-0870-5

Song Y, Ma MG, Veroustraete F (2010) Comparison and conversion of AVHRR GIMMS and SPOT VEGETATION NDVI data in China. Int J Remote Sens 31:2377–2392. https://doi.org/10.1080/01431160903002409

Steduto P, Hsiao TC, Fereres E (2007) On the conservative behavior of biomass water productivity. Irrig Sci 25:189–207. https://doi.org/10.1007/s00271-007-0064-1

Swann A, Fung I (1998) Assessing models of respiration using Fluxnet nighttime NEE. Fortune 137:159–160

Toft NL, Anderson JE, Nowak RS (1989) Water use efficiency and carbon isotope composition of plants in a cold desert environment. Oecologia 80:11–18. https://doi.org/10.1007/BF00789925

Tong XJ, Zhang JS, Meng P, Li J, Zheng N (2014) Ecosystem water use efficiency in a warm-temperate mixed plantation in the North China. J Hydrol 512:221–228. https://doi.org/10.1016/j.jhydrol.2014.02.042

Torres-García W, Domenech M (2017) Hedgehog-mesenchyme gene signature identifies bi-modal prognosis in luminal and basal breast cancer sub-types. Mol BioSyst 13:2615–2624. https://doi.org/10.1039/c7mb00416h

Troch PA, Martinez GF, Pauwels VRN et al (2009) Climate and vegetation water use efficiency at catchment scales. Hydrol Process 23:2409–2414. https://doi.org/10.1002/hyp.7358

Wang GY, Innes JL, Lei JF, Dai SY, Wu SW (2007) China's forestry reforms. Science 318:1556–1557. https://doi.org/10.1126/science.1147247

Wang YL, Zhou GS, Wang YH (2008) Environmental effects on net ecosystem CO_2 exchange at half-hour and month scales over *Stipa krylovii* steppe in northern China. Agric For Meteorol 148:714–722. https://doi.org/10.1016/j.agrformet.2008.01.013

Wang XP, Brown-Mitic CM, Kang ES, Zhang JG, Li XR (2010) Evapotranspiration of *Caragana korshinski* communities in a revegetated desert area: Tengger Desert, China. Hydrol Process 18: 3293–3303. https://doi.org/10.1002/hyp.5661

Wei SH, Yi CX, Fang W, Hendrey G (2017) A global study of GPP focusing on light-use efficiency in a random forest regression model. Ecosphere 8(5):e01724. https://doi.org/10.1002/ecs2.1724

Wilson KB, Baldocchi DD, Aubinet M et al (2002) Energy partitioning between latent and sensible heat flux during the warm season at FLUXNET sites. Water Resour Res 38:30-31–30-11. https://doi.org/10.1029/2001WR000989

Wohlfahrt G, Fenstermaker LF, Arnone IJA (2008) Large annual net ecosystem CO_2 uptake of a Mojave Desert ecosystem. Glob Chang Biol 14:1475–1487. https://doi.org/10.1111/j.1365-2486.2008.01593.x

Xie J, Zha TS, Zhou CX et al (2016) Seasonal variation in ecosystem water use efficiency in an urban-forest reserve affected by periodic drought. Agric For Meteorol 221:142–151. https://doi.org/10.1016/j.agrformet.2016.02.013

Xu LK, Baldocchi DD (2004) Seasonal variation in carbon dioxide exchange over a Mediterranean annual grassland in California. Agric For Meteorol 123:79–96. https://doi.org/10.1016/j.agrformet.2003.10.004

Yang YH, Fang JY, Fay PA, Bell JE, Ji CJ (2010) Rain use efficiency across a precipitation gradient on the Tibetan Plateau. Geophys Res Lett 37:78–82. https://doi.org/10.1029/2010GL043920

Yang HT, Li XR, Wang ZR, Jia R, Liu L, Chen Y, Wei Y, Gao Y, Li G (2014) Carbon sequestration capacity of shifting sand dune after establishing new vegetation in the Tengger Desert, northern China. Sci Total Environ 478:1–11. https://doi.org/10.1016/j.scitotenv.2014.01.063

Zhang D, Jin TT (2016) Variations of water-carbon exchange at leaf scale and leaf nutrient content of Robinia pseudoacacia with slope aspect and stand age in a small catchment of the Loess Plateau. Chin J Ecol 35:354–362. https://doi.org/10.13292/j.1000-4890.201602.034 (in Chinese)

Zhang ZS, Li XR, Wang T, Wang XP, Xue QW, Liu LC (2008) Distribution and seasonal dynamics of roots in a revegetated stand of *Artemisia ordosica Kracsh*. in the Tengger Desert (North China). Arid Land Res Manag 22:195–211. https://doi.org/10.1080/15324980802182980

Zhang ZS, Li XR, Liu LC, Jia RL, Zhang JG, Wang T (2009) Distribution, biomass, and dynamics of roots in a revegetated stand of *Caragana korshinskii* in the Tengger Desert, northwestern China. J Plant Res 122:109–119. https://doi.org/10.1007/s10265-008-0196-2

Zhang T, Zhang YJ, Xu MJ et al (2018) Water availability is more important than temperature in driving the carbon fluxes of an alpine meadow on the Tibetan Plateau. Agric For Meteorol 256–257:22–31. https://doi.org/10.1016/j.agrformet.2018.02.027

Zhao MS, Running SW (2010) Drought-induced reduction in global terrestrial net primary production from 2000 through 2009. Science 329:940–943. https://doi.org/10.1126/science.1192666

Zhao FH, Yu GR, Li SG et al (2007) Canopy water use efficiency of winter wheat in the North China plain. Agric Water Manag 93:99–108. https://doi.org/10.1016/j.agwat.2007.06.012

Zhu ZL, Sun XM, Wen XF, Zhou YL, Tian J, Yuan GF (2006) Study on the processing method of nighttime CO_2 eddy covariance flux data in ChinaFLUX. Sci China Ser D 49:36–46. https://doi.org/10.1007/s11430-006-8036-5

Zhu XJ, Yu GR, Wang QF et al (2015) Spatial variability of water use efficiency in China's terrestrial ecosystems. Glob Planet Chang 129: 37–44. https://doi.org/10.1016/j.gloplacha.2015.03.003